Jurnal Teknologi

Full Paper

PERFORMANCE ASSESSMENT OF A SOLID DESICCANT AIR DEHUMIDIFIER

Nazri Kamsah[a], Haslinda Mohamed Kamar[a*], Muhammad Imran Wan Khairuzzaman[a], M. Idrus Alhamid[b], Fazila Mohd Zawawi[a]

[a]Faculty of Mechanical Engineering Universiti Teknologi Malaysia, 81310 UTM Johor Bahru, Johor, Malaysia
[b]Departemen Teknik Mesin, Fakultas Teknik, Universitas Indonesia, Kampus Baru – UI, Depok, 16424, Indonesia

Article history
Received
1 January 2016
Received in revised form
18 May 2016
Accepted
15 June 2016

*Corresponding author
haslinda@mail.fkm.utm.my

Graphical abstract

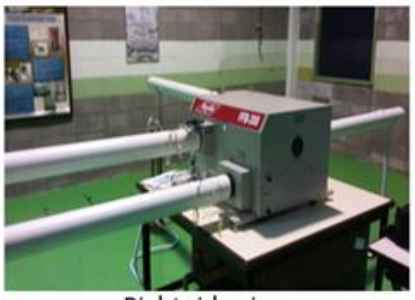

Right side view

Abstract

The presence of moisture in the air along with temperature has a long term and devastating effect on man and material. One way to create a low humidity environment is by using a solid desiccant wheel system. In the present work, an experimental analysis has been carried out under steady-state conditions to investigate the effects of different operating parameters on a solid desiccant wheel system performances. An experimental rig consists of an FFB300 air dehumidifier system was constructed. A parametric investigation was carried out to examine the effects of the reactivation air inlet temperature and process air outlet velocity on the thermal effectiveness, dehumidification efficiency, and moisture removal rate of the desiccant wheel system. The analysis shows that both thermal effectiveness and dehumidification efficiency decrease with the increase of the reactivation air inlet temperature, by 2.5 % and 43 %, respectively. Likewise, when the process air outlet velocity increases both performances criteria reduce by 10 % and 28 %, respectively. The moisture removal rate increases significantly by 30 % as the reactivation air inlet temperature increases. However, the process air outlet velocity has no significant effect on the moisture removal rate.

Keywords: Solid desiccant system; regeneration temperature; process air outlet velocity

Abstrak

Kehadiran wap air dalam udara dan suhu udara mempunyai kesan jangka panjang yang merosakkan manusia dan bahan. Satu cara untuk menghasilkan sekitaran yang berkelembapan rendah adalah dengan menggunakan sistem ejen pengering jenis pejal. Dalam kajian ini, analisa ujikaji dalam keadaan mantap telah dilakukan untuk menyelidik kesan parameter operasi yang berbeza ke atas prestasi sistem roda bahan pengering. Pelantar ujikaji yang terdiri daripada sebuah sistem pengering udara model FFB300 telah dibangunkan. Kajian parameter telah dibuat untuk menyiasat kesan suhu masukan udara pengaktifan semula dan halaju keluaran udara proses ke atas keberkesanan terma, kecekapan pengeringan dan kadar pembuangan lembapan sistem roda ejen pengering. Keputusan kajian menunjukkan bahawa keberkesanan terma dan kecekapan pengeringan menurun dengan peningkatan suhu masukan udara pengaktifan semula, masing-masing, sebanyak 2.5% dan 43%. Begitu juga, apabila halaju keluaran udara proses ditingkatkan, kedua-dua ciri prestasi berkurang, masing-masing, sebanyak 10% dan 28%. Kadar penyahlembapan udara meningkat sebanyak 30% apabila suhu masukan udara pengaktifan semula ditingkatkan. Walau bagaimanapun, halaju keluaran udara proses tidak memberi kesan ketara ke atas kadar pembuangan kelembapan udara.

Kata kunci: Sistem ejen pengering pejal; suhu pengaktifan semula; halaju keluaran udara proses

1.0 INTRODUCTION

Humidity is just a tiny amount of moisture which cannot be seen or felt but always exist in the surrounding air. The presence of moisture in the air along with temperature has a long term and destructive effect on man, machine and material in many industries. The damage which can be caused by excessive humidity are, corrosion of steel and metals, deteriorated characteristics of the hygroscopic material and increased the harmful activity of microorganisms. Some industrial processes are very sensitive to moisture, and they require environments with extremely low humidity. One of the examples is lithium-ion battery manufacturing processes, where they are carried out in dry rooms where the local microenvironment must be controlled to preserve optimum production conditions.

One way to create this extremely low humidity environment is by using a solid desiccant wheel system. The solid desiccant wheel system consists of a cylindrical matrix of channels that are constructed from a solid desiccant. To maximizing moisture collection, the wheel rotates slowly through two air streams. "Process" air passes through one section of the wheel. Desiccant on that section adsorbs water vapor, making the air drier than when it entered. Wheel rotation then exposes the moisture-laden desiccant to a "regenerating" air stream that strips the captured moisture away from the desiccant [1]. The most important component of the desiccant wheel system is the desiccant materials. Its structural configuration, thermal capacity and sorption characteristics largely control the operating economics of the desiccant system. Ideally, the desiccant should have infinitely small mass and infinitely high surface area. Due to low mass minimizes the amount of energy wasted in heating and cooling the desiccant, and large surface area maximizes the interaction between the desiccant and the surrounding air [2]. The issue is, how to establish an effective desiccant system for creating an adequately low humidity environment without compromising its operating economy, system efficiency and durability of desiccant wheel configurations.

Many studies have been conducted either by experimental or numerical modelling to assess desiccant performances [2 & 3]. The most productive research is directing towards improving the cost-benefit ratio of desiccant equipment for respective applications [2]. Some focused areas that have been reported in the literature are, studies of sorption phenomena [4]; prediction and determination of sorption dynamics [5]; determination of desired optimum desiccant properties [6]; develop simulation models with different desiccant materials [7-10]; determine optimal operating strategies at various conditions [11, 13-15]; analyze the applications of using alternative fuels and the possibilities of using waste heat for desiccant systems [16-20]; develop wheels with composite desiccants [5-7] and last but not least study heat and mass transfer enhancement for desiccant systems [3, 21-23]. The recent research activities on the desiccant technology are very encouraging.

A comprehensive approach is required for examining solid desiccant systems accurately. One of the methods is by performing experiment activities. In the present work, an experimental analysis has been carried out to investigate the effects of different operating parameters on the solid desiccant wheel system performances. An experimental rig consists of an FFB300 air dehumidifier system was constructed. The influences of reactivation air inlet temperature and process air inlet velocity on the system performances were analyzed.

2.0 METHODOLOGY

2.1 Operating Principle of a Desiccant Wheel

The desiccant dehumidifier has two separate primary air streams, process and reactivation streams as shown in Figure 1. The humid process air passes through a dehumidification section approximated 75% of the honeycomb rotor (desiccant wheel) face area. The rotor is made of silica gel that capable of absorbing water molecules results in the dehumidification of moisture in the air after it traverses the rotor.

Simultaneously the reactivation air is heated before passing through a reactivation section estimated 25% of the rotor surface area. The silica gel gives away the moisture to the hot air stream as a result of evaporation of the water molecule. The warm and humid air then is exhausted from the desiccant dehumidifier.

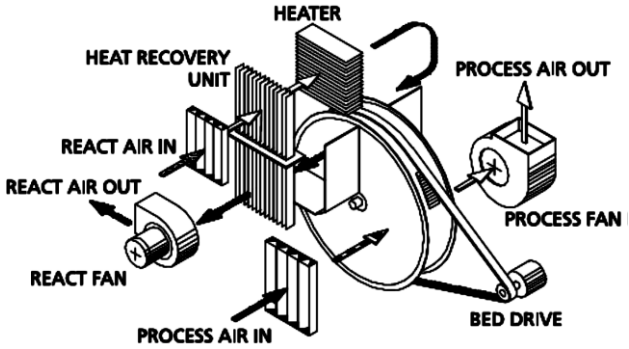

Figure 1 Working principle of a desiccant wheel [23].

In this manner, the desiccant wheel restores its capacity to absorb water molecules from fresh incoming process air. While recovering the performance of the rotor, the reactivation air stream also washes the surface of the rotor from undesirable particles. A continuous rotation of the rotor provides an ongoing process of adsorption/reactivation. Individual holding frame from both sides of the desiccant wheel prevents the mixing of the process and the reactivation air streams.

The air dehumidification process of the desiccant wheel can be clearly illustrated on a psychrometric chart as shown in Figure 2. The inlets and outlets of the process and reactivation air streams are denoted as 1, 2', 3 and 4', respectively. Process 1 to 2' represents the actual path of the process air and 3 to 4' expresses the real process of the reactivation air. The ideal process of the process and reactivation air streams can be considered as an isenthalpic process [19] as shown by lines 1 to 2 and 3 to 4, respectively. The moist process air enters the dehumidification section at state 1.

After it passes through the desiccant wheel (state 2'), its temperature increases and its specific humidity decreases because the desiccant draws the water molecules in the air until it is saturated. In a different air stream, the hot reactivation air enters the reactivation section at state 3, to heat up the saturated desiccant thus releases the moisture through the evaporation of the water molecules. The warm and humid air then routed out from the wheel at state 4'

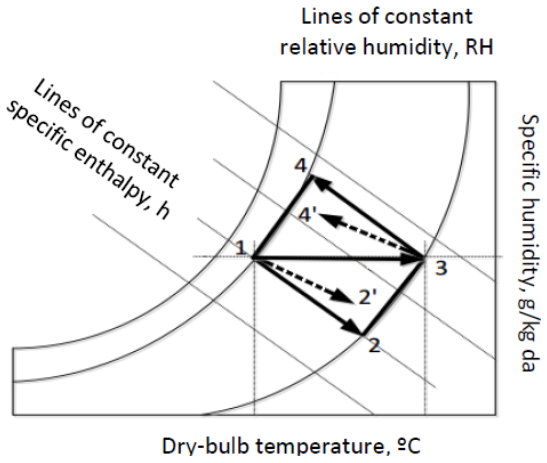

Figure 2 Sketch of process paths on the psychrometric chart

2.2 System Description

The test rig consists of a solid desiccant air dehumidifier (SDAD) unit, model FFB-300 furnished with PVC pipes of 1200 mm length and 100 mm diameter to facilitate regulating the conditions of air at each inlet and outlet of the reactivation and process sections, respectively. Figures 3 and 4 show the schematic diagram of the test rig and the original test apparatus arrangement, respectively. The main components of the SDAD system included a regeneration fan, process fan, heat recovery unit, heater, solid desiccant wheel powder coated finish and incorporates a high performance fluted metal silicate desiccant synthesized rotor, and bed drive. The reactivation air temperature was regulated using a proportional integral derivative (PID) controller. The PID controller is a control loop feedback mechanism which consistently estimates an error value i.e. the difference between the air temperatures of the desired reactivation set point and the measured values. The controller attempts to reduce the error over time by correcting the power supplied to the heater. To provide variation of process air velocity at the inlet, the process fan speed was controlled using a reducer unit and damper.

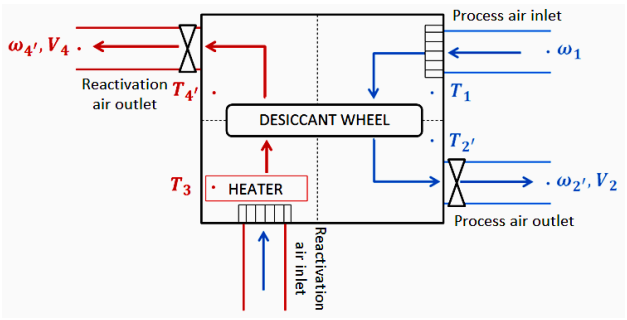

Figure 3 The schematic diagram of the test rig.

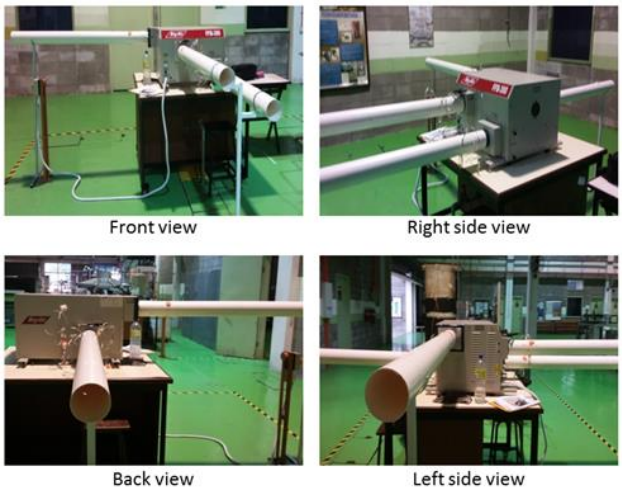

Figure 4 The test apparatus arrangement.

The test apparatus of the SDAD system was fully instrumented to record and control the operating parameters such as the reactivation air temperature and process air velocity. Four K-type thermocouples with an accuracy of ±0.1°C were used to measure the air temperature at each inlet and outlet of the reactivation and process air streams. The thermocouples have been calibrated using a standard thermometer with an error of ±0.02%. A Pitot tube anemometer model EXTECH HD350 with an accuracy of ±0.1 m/s was used to measure the velocity of the process air. The air humidity at each inlet and outlet was measured using a digital hygrometer model TES 1364 with an accuracy of ±0.3%. The latter two devices were newly purchased. Therefore, the calibrations have been carried out by the manufacturers.

2.3 Experimental Procedures

The experimental work was conducted at steady-state conditions. The tests were run at different reactivation air temperatures by regulating the PID controller. The power supplied to the reactivation heater that creates the variation of reactivation air temperature, has to be limited. Because of the continuous operation of the system during the experiment, the heater can only be operated at temperatures lower than 70°C. Due to this, the reactivation air temperature, T_3, can only be set at 40, 50, and 60°C. At each temperature, the process air flowing through the dehumidification section was set between 6.5 and 9.5 m/s using a reducer unit and damper. For each variation, the process air inlet temperature, T_1, process air inlet specific humidity, ω_1, reactivation air inlet specific humidity, ω_3, process air outlet temperature, $T_{2'}$, and process air outlet specific humidity, $\omega_{2'}$, were obtained. For stabilizing the SDAD system, it was left running 30 minutes before each test. Table 1 summarizes the input variables, output variables and the performance criteria of the solid desiccant system.

Table 1 Parametric analysis

Input Parameters	Output Parameters	Performance Criteria
1. Reactivation air inlet temperature, T_3 ~ 40 to 60°C 2. Process air inlet velocity, $\bar{V}_{2'}$ ~ 6.5 to 9.5 m/s	1. Process air inlet temperature, T_1 (°C) 2. Process air inlet specific humidity, ω_1 (g/kg da) 3. Reactivation air inlet specific humidity, ω_3 (g/kg da) 4. process air outlet temperature, $T_{2'}$ (°C) 5. process air outlet specific humidity, $\omega_{2'}$ (g/kg da)	1. Thermal effectiveness, $\varepsilon_t = \frac{(T_{2'}-T_1)}{(T_3-T_1)}$ 2. Dehumidification efficiency(%), $\eta_{Dh} = \frac{(\omega_1-\omega_{2'})}{(\omega_1-\omega_{2,ideal})}$ 3. Moisture removal rate (g/s), $\dot{m}_w = \dot{m}_a(\omega_1-\omega_{2'}) = \rho\bar{V}A(\omega_1-\omega_{2'})$*

* ρ = density of the air, kg/m³; $\bar{V}$= process air velocity, m/s; A = cross sectional area of the pipe, m²

A complete uncertainty analysis was performed which involves a comprehensive identification of all sources of uncertainty that contribute to the joint probability distributions of each input and output variables. Table 2 outlines the uncertainties for different parameters.

Table 2 Uncertainty values for different parameters

Parameters	Minimum Error (%)	Maximum Error (%)
Process air inlet velocity, $\bar{V}$	0.6	1.4
Process air inlet temperature, T_1	0.03	0.15
Process air outlet temperature, $T_{2'}$	0.11	0.5
Process air inlet relative humidity, RH_1	0.14	0.5
Process air outlet relative humidity, RH_2	0.18	1
Process air inlet specific humidity, ω_1	0.14	0.5
Process air outlet specific humidity, $\omega_{2'}$	0.2	0.6
Thermal effectiveness, ε_t	1.6	4
Dehumidification efficiency, η_{Dh}	3.6	14.2
Moisture removal rate, $\dot{m}_w$	3.9	13.8

2.4 Performance Criteria of a Solid Desiccant Wheel

A solid desiccant wheel is designed for the purpose of producing a low humidity environment, and its performance is expressed in terms of thermal effectiveness, ε_t, dehumidification efficiency, η_{Dh}, and moisture removal rate, $\dot{m}_w$. The thermal effectiveness as expressed in Equation (1) is defined as the ratio between the temperature of the process

air and the maximum available temperature difference across the wheel.

$$\varepsilon_t = \frac{(T_{2'} - T_1)}{(T_3 - T_1)} \quad (1)$$

The dehumidification efficiency measures the deviation of actual desiccant wheel performance from the idealized isenthalpic behavior [3] and is described in Equation (2).

$$\eta_{Dh} = \frac{(\omega_1 - \omega_{2'})}{(\omega_1 - \omega_{2,ideal})} \quad (2)$$

While the moisture removal rate of the process air is derived from the mass balance analysis on the wheel and is shown in Equation (3).

$$\dot{m}_w = \dot{m}_a(\omega_1 - \omega_{2'}) = \rho A_c \bar{V}(\omega_1 - \omega_{2'}) \text{ (kg/s)} \quad (3)$$

where T and ω are the temperature and specific humidity of the air, respectively. While ρ, $\bar{V}$ and A_c are the air density, air velocity and cross sectional area of the ducting pipes, respectively.

During the analysis, several assumptions are adopted as follows:

1. The wheel experiences a steady-flow process and thus the mass flow rate of dry air remains constant during the entire process.
2. Dry air and the water vapor are ideal gases.
3. The kinetic and potential energy changes are negligible.
4. The air flow is a one dimensional flow.

3.0 RESULTS AND DISCUSSION

The performance criteria described in Equation (1) through Equation (3) are evaluated for various values of reactivation air inlet temperature, T_3, and process air inlet velocity, $\bar{V}_{2'}$. The results of the parametric analysis are tabulated in Table 3 and illustrated in Figures 5 to 10.

Table 3 The thermal effectiveness, dehumidification efficiency and moisture removal rate for the desiccant wheel of various reactivation air inlet temperature and process air outlet velocity.

T_3 (°C)	$\bar{V}_{2'}$ (m/s)	ε_t	η_{Dh} (%)	$\dot{m}_w$ (g/s)
40	6.77 ± 0.04	43.03 ± 1.03	68.02 ± 9.66	0.071 ± 0.008
	7.52 ± 0.06	38.66 ± 1.24	59.25 ± 7.20	0.070 ± 0.008
	8.69 ± 0.08	39.01 ± 1.12	64.57 ± 8.30	0.082 ± 0.008
	9.37 ± 0.10	32.59 ± 1.47	48.31 ± 6.85	0.068 ± 0.009
50	6.75 ± 0.06	41.82 ± 1.31	51.09 ± 4.69	0.119 ± 0.010
	7.20 ± 0.06	40.89 ± 1.63	53.16 ± 3.93	0.141 ± 0.009
	8.55 ± 0.06	36.20 ± 0.82	46.12 ± 3.71	0.132 ± 0.010
	9.41 ± 0.13	34.08 ± 1.06	35.31 ± 5.13	0.123 ± 0.017
60	6.48 ± 0.04	41.79 ± 1.03	42.48 ± 3.93	0.161 ± 0.014
	7.86 ± 0.05	38.35 ± 0.69	36.53 ± 1.33	0.178 ± 0.007
	8.53 ± 0.04	36.23 ± 0.58	24.71 ± 1.96	0.132 ± 0.011
	9.35 ± 0.06	33.27 ± 0.70	30.88 ± 2.43	0.182 ± 0.014

The effects of the reactivation air inlet temperature, T_3 on the thermal effectiveness, ε_t are illustrated in Figure 5. Where the thermal effectiveness is plotted against the reactivation air inlet temperature. The rate of decline in ε_t varies over the range of T_3. The thermal effectiveness drops slightly from 40 to 50°C, but from 50 to 60°C the decline is steeper. Overall, there is a reduction in ε_t of about 2.5 %. A desiccant wheel with a higher efficiency clearly saves a greater amount of energy since the inlet reactivation air requires fewer amount of heat to increase its temperature before passing through the wheel.

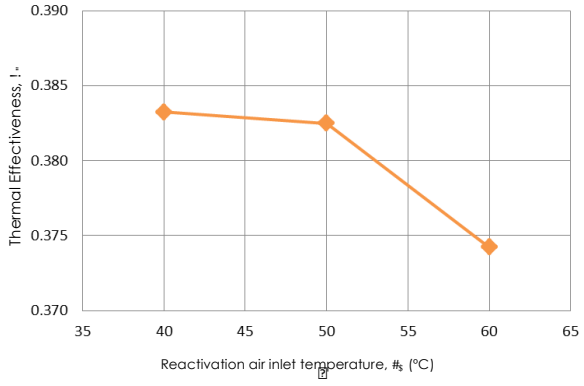

Figure 5 The variation of the reactivation air inlet temperature with thermal effectiveness.

A plot of dehumidification efficiency, η_{Dh} versus reactivation air inlet temperature, T_3 is shown in Figure 6. It is evident from the figure as T_3 increases η_{Dh} drops. Thus, reactivation air inlet at higher temperature increases the deviation of actual desiccant wheel performance from the idealized isenthalpic behavior, as described in Equation (2). The dehumidification efficiency decline steadily over the range of T_3 by about 43%.

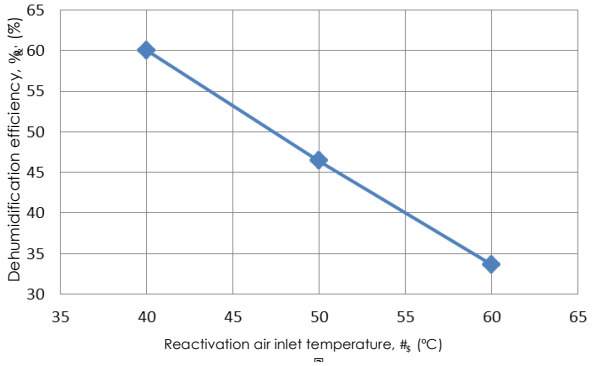

Figure 6 Variation of dehumidification efficiency as the reactivation air inlet increases from 40 to 60°C.

The effects of the process air outlet velocity, $\bar{V}_{2'}$ on the thermal effectiveness, ε_t is illustrated in Figure 7. Where ε_t is plotted against $\bar{V}_{2'}$ and it can be found that an increase in $\bar{V}_{2'}$ will reduce ε_t. It can also be seen that the curve presents a linear trend. Overall, there is a reduction in the thermal effectiveness of about 10%. It can also be concluded that, by observing Equation (1), the process air outlet velocity has somewhat influenced the temperature of process air, $T_{2'}$ at the wheel outlet.

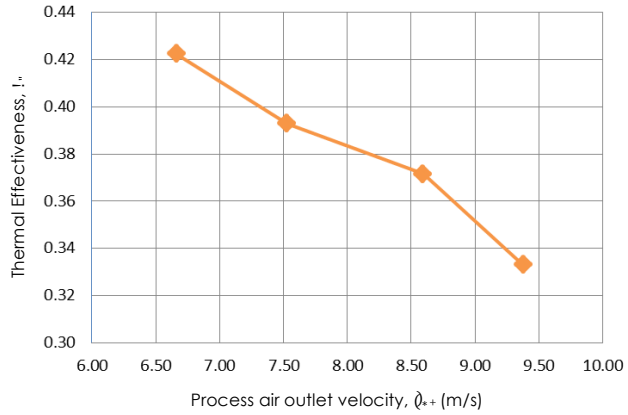

Figure 7 The variation of the thermal effectiveness with process air outlet velocity.

Figure 8 illustrates the variation of the dehumidification efficiency, η_{Dh} with the process air outlet velocity, $\bar{V}_{2'}$. The plot represents the results of the calculations acquired from Equation (2). It can be seen that as the process air outlet velocity increases, the dehumidification efficiency drops considerably. Higher outlet velocity of the process air degrades the possible of the actual desiccant wheel behavior to obtain its idealized performance. As $\bar{V}_{2'}$ increases from 6.5 m/s to 9.5 m/s, η_{Dh} decreases by 28 %. This finding is found to be in good agreement with the study reported by De Antonellis et al. [24].

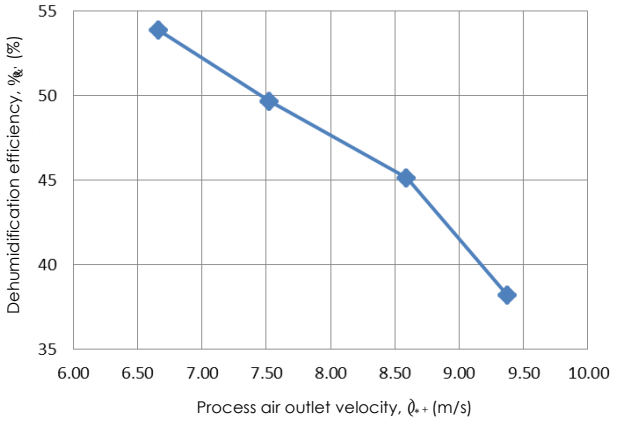

Figure 8 The variation of the thermal effectiveness with process air outlet velocity.

Figure 9 shows the effects of reactivation air inlet temperature, T_3 on the moisture removal rate, $\dot{m}_w$ of the process air. A significant increase in the moisture removal rate as the reactivation air inlet temperature increases. This finding shows that the desiccant wheel improves its performance of removing moisture from the process air that passes through it when T_3 is increased. The moisture removal rate increase steadily over the range of T_3 by about 30 %. The trend of the plotted curve agrees well with the work done by Ali et al. [23].

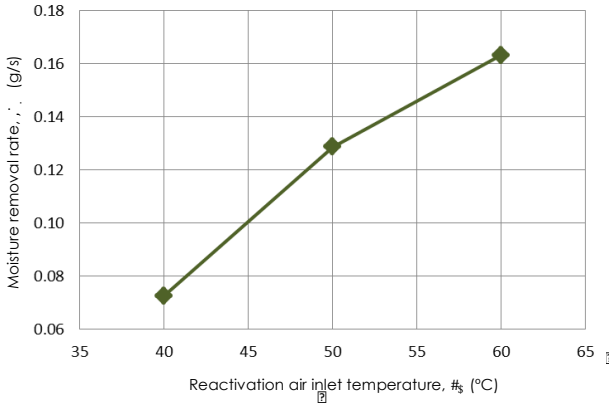

Figure 9 Effects of the reactivation air inlet temperature on moisture removal rate.

Figure 10 shows the variation of the moisture removal rate of the process air, $\dot{m}_w$ with the process air outlet velocity, $\bar{V}_{2'}$. It can be observed that the moisture removal rate remains relatively constant in a range between 0.10 g/s and 0.15 g/s as the process air outlet velocity increases from 6.5 m/s to 9.5 m/s. This finding shows that the process air outlet velocity has no significant effect on the moisture removal rate. This result agrees with the conclusions described in Yadav and Bajpai [11].

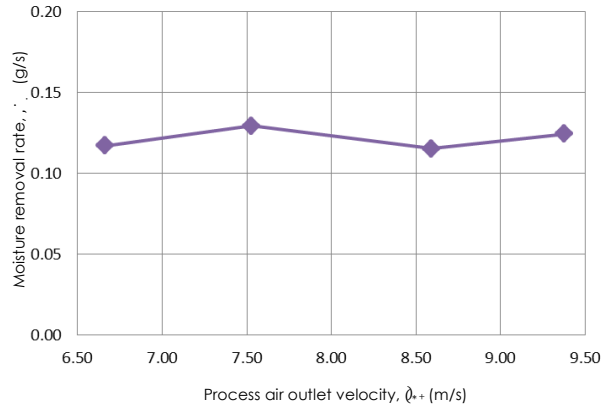

Figure 10 Effects of process air outlet velocity on dehumidification rate.

4.0 CONCLUSION

In this study, experiments were carried out on a solid desiccant air dehumidifier model FBB 300. The aim was to examine the effects of varying reactivation air inlet temperature and process air velocity on the thermal effectiveness, dehumidification efficiency and moisture removal rate of the air dehumidifier unit. It was found that both the thermal effectiveness and dehumidification efficiency drop as the reactivation air inlet temperature increases. Over the range of the reactivation air temperature, both performances criteria fall by 2.5 % and 43 %, respectively. The rate of

reduction in the thermal effectiveness is slightly smaller than that of the dehumidification efficiency. However, the moisture removal rate increases significantly by 30 % as the reactivation air inlet temperature increases. The same trends are observed for both thermal effectiveness and dehumidification efficiency as the process air inlet velocity increases. Across the range of the process air outlet velocity, the performance criteria drop by 10 % and 28 %, respectively. However, the process air outlet velocity has no significant effect on the moisture removal rate.

Acknowledgement

This research is fully supported by FRGS grant, Vote number 4F645. The authors fully acknowledged Ministry of Higher Education (MOHE) and Universiti Teknologi Malaysia for the approved fund which makes this important research viable and effective.

References

[1] Advances in Desiccant-Based Dehumidification: Trane retrieved February, 01, 2016 from https://www.trane.com/content/dam/Trane/Commercial/global/products-systems/education-training/engineers-newsletters/airside-design/admapn016en_0905.pdf.

[2] Mei V. C., Chen F. C., Lavan Z., Collier R. K. and Meckler, G. 1992. An Assessment of Desiccant Cooling and Dehumidification Technology. Oak Ridge National Laboratory Desiccant Cooling: Oak Ridge: Tennessee, USA.

[3] Zhang X. J., Dai Y. J. and Wang R. Z. 2003. A Simulation Study of Heat and Mass Transfer in a Honeycombed Rotary Desiccant Dehumidifier. *Applied Thermal Engineering*. 23(8): 989-1003.

[4] Cui, Q., Chen, H., Tao, G., and Yao, H. 2005. Performance Study of New Adsorbent for Solid Desiccant Cooling. *Energy*. 30(2): 273-279.

[5] Zhang, X. J., Sumathy, K., Dai, Y. J., and Wang, R. Z. 2005. Parametric Study on the Silica Gel–calcium Chloride Composite Desiccant Rotary Wheel Employing Fractal BET Adsorption Isotherm. *International Journal of Energy Research*. 29(1): 37-51.

[6] Golubovic, M. N., Hettiarachchi, H. D. M., and Worek, W. M. 2006. Sorption Properties for Different Types of Molecular Sieve and their Influence on Optimum Dehumidification Performance of Desiccant Wheels. *International Journal of Heat and Mass Transfer*. 49(17): 2802-2809.

[7] Ge, T. S., Ziegler, F., and Wang, R. Z. 2010. A Mathematical Model for Predicting the Performance of a Compound Desiccant Wheel (A Model of Compound Desiccant Wheel). *Applied Thermal Engineering*. 30(8): 1005-1015.

[8] Kadoli R. and Babu T.A. 2011. Improved Utilization of Desiccant Material in Packed Bed Dehumidifier Using Composite Particles. *Renewable Energy*. 36(2): 732-742.

[9] Chih-Hao Chen, Chien-Yeh Hsu, Chih-Chieh Chen and Sih-Li Chen. 2015. Silica Gel Polymer Composite Desiccants for Air Conditioning Systems. *Energy and Buildings*. 101: 122–132.

[10] Li-Zhi Zhang, Huang-Xi Fu, Qi-Rong Yang and Jian-Chang Xu. 2014. Performance Comparisons of Honeycomb-type Adsorbent Beds (wheels) for Air Dehumidification with Various Desiccant Wall Materials. *Energy*. 65: 430-440.

[11] De Antonellis, S., Joppolo C.M. and Molinaroli L. 2010. Simulation, Performance Analysis and Optimization of Desiccant Wheels. *Energy and Buildings*. 42(9): 1386-1393.

[12] Yadav, Avadhesh, and Bajpai, V. K. 2011. Optimization of Operating Parameters of Desiccant Wheel for Rotation Speed. *International Journal of Advanced Science and Technology*. 32: 109-116.

[13] Ahmed M.H., Kattab N.M. and Fouad M. 2005. Evaluation and Optimization of Solar Desiccant Wheel Performance. *Renewable Energy*. 30(3): 305-325.

[14] Ruivo, C. R., and Angrisani, G. 2014. The Effectiveness Method to Predict the Behavior of a Desiccant Wheel: An Attempt of Experimental Validation. *Applied Thermal Engineering. 71*(2): 643-651.

[15] Ramzy A., Abdel Meguid H. and ElAwady W.M. 2015. A Novel Approach for Enhancing the Utilization of Solid Desiccants in Packed Bed via Intercooling. *Applied Thermal Engineering*. 78: 82-89.

[16] Myat A., Thu K. and Choon N.K. 2012. The Experimental Investigation on the Performance of a Low Temperature Waste Heat-driven Multi-bed Desiccant Dehumidifier (MBDD) and Minimization of Entropy Generation. *Applied Thermal Engineering*. 39: 70-77.

[17] Zhao Y., Dai Y.J., Ge T.S., Wang H.H. and Wang R.Z. 2016. A High Performance Desiccant Dehumidification Unit Using Solid Desiccant Coated Heat Exchanger with Heat Recovery. *Energy and Buildings*. Accepted Manuscript: 2016 January 19.

[18] Tu R., Liu X.H. and Jiang Y. 2013. Performance Analysis of a New Kind of Heat Pump-driven Outdoor Air Processor Using Solid Desiccant. *Renewable Energy*. 57: 101-110.

[19] Wang H.H., Ge T.S., Zhang X.L. and Zhao Y. 2016. Experimental Investigation on Solar Powered Self-cooled Cooling System Based on Solid Desiccant Coated Heat Exchanger. *Energy*. 96: 176-186.

[20] Guan Y., Zhang Y., Sheng Y., Kong X. and Du S. 2015. Feasibility and Economic Analysis of Solid Desiccant Wheel Used for Dehumidification and Preheating in Blast Furnace: A Case Study of Steel Plant, Nanjing, China. *Applied Thermal Engineering*. 81, 426-435.

[21] Wang N., Zhang J. and Xia X. 2013. Desiccant Wheel Thermal Performance Modelling for Indoor Humidity Optimal Control. *Applied Energy*. 112: 999-1005.

[22] Ruivo, C., Costa, J., and Rui, A. 2011. Heat and Mass Transfer in Desiccant Wheels. *Advanced Topics in Mass Transfer*.

[23] Chua, K. J. 2015. Heat and Mass Transfer of Composite Desiccants for Energy Efficient Air Dehumidification: Modelling and Experiment. *Applied Thermal Engineering*. 89: 703-716.

[24] Bry Air. Dehumidification. 2015. Applications Engineering Manual.

[25] Ali, M., Vukovic, V., Sahir, M.H., Basciotti, D. 2013. Development and Validation of Desiccant Wheel Model Calibrated under Transient Operating Conditions. *Applied Thermal Engineering*. 61: 469-480.

[26] Stefano De Antonellis, Manuel Intini, Cesare Maria Joppolo, and Federico Pedranzini. 2014. Experimental Analysis and Practical Effectiveness Correlations of Enthalpy Wheels. *Energy and Buildings*. 84: 316–323.